

Assessing antenna field of view and receiver clocks of COSMIC and GRACE satellites: lessons for COSMIC-2

Tzu-Pang Tseng · Kefei Zhang · Cheinway Hwang ·
Urs Hugentobler · Chuan-Sheng Wang ·
Suelynn Choy · Yi-Shan Li

Received: 27 February 2012 / Accepted: 8 March 2013 / Published online: 3 April 2013
© Springer-Verlag Berlin Heidelberg 2013

Abstract We provide suggestions for the approved COSMIC-2 satellite mission regarding the field of view (FOV) and the clock stability of its future GNSS receiver based on numerical analyses using COSMIC GPS data. While the GRACE GPS receiver is mounted on the zenith direction, the precise orbit determination (POD) antennas of COSMIC are not. The COSMIC antenna design results in a narrow FOV and a reduction in the number of GPS observations. To strengthen the GPS geometry, GPS data from two POD antennas of COSMIC are used to estimate its orbits. The phase residuals of COSMIC are at the centimeter level, compared to the millimeter level of GRACE. The receiver clock corrections of COSMIC and GRACE are at the microsecond and nanosecond levels, respectively. The clock spectra of COSMIC at the frequencies of 0–0.005 Hz contain significant powers, indicating potential systematic errors in its clock corrections. The clock stability, expressed by the Allan deviation, of COSMIC ranges from 10^{-9} to 10^{-11} over 1 to 10^4 s, compared to 10^{-12}

to 10^{-14} for GRACE. Compared to USO-based clock of GRACE, the clock of COSMIC is degraded in its stability and is linked to the reduction of GPS data quality. Lessons for improvement of COSMIC-2 over COSMIC in FOV and receiver clock stability are given.

Keywords Clock stability · COSMIC · Field of view · GPS · Precise orbit determination

Introduction

The Constellation Observing System for Meteorology, Ionosphere and Climate (COSMIC) mission consists of six microsatellites, named FM1-FM6, and was launched in April 2006 (Fong et al. 2008). Each satellite is equipped with four antennas connected to one GPS receiver (Fig. 1). Two signal-patch antennas for precise orbit determination (POD) are mounted on the upper part of the satellite body, and the other two antennas for radio occultation (GPS-RO) research are mounted on the bottom part. The POD antenna boresight vector is tilted by 75° toward the flight direction (Hwang et al. 2010). One of the two POD antennas is called the default antenna and is able to receive signals from more than four GPS satellites for POD. The non-default antenna cannot track more than four GPS satellites due to the limited channels of the COSMIC receiver. The COSMIC orbit accuracy using data from the default antenna was assessed by Hwang et al. (2009, 2010) and Tseng et al. (2012) using orbit overlap, applying phase center variation (PCV), and GPS signal quality and satellite attitude quality information.

The GPS occultation receiver onboard a COSMIC satellite is called integrated GPS occultation receiver (IGOR). Like the BlackJack GPS receiver on GRACE, the IGOR was also designed by Jet Propulsion Laboratory

T.-P. Tseng
GPS Science and Application Research Center, National Central University, 300 Zhongda Road, Jhongli City 32001, Taiwan

T.-P. Tseng · K. Zhang · C.-S. Wang · S. Choy
SPACE Research Centre, Royal Melbourne
Institute of Technology (RMIT) University,
394-412 Swanston Street, Melbourne 3001, Australia

C. Hwang (✉) · Y.-S. Li
Department of Civil Engineering, National Chiao Tung University, 1001 University Road, Hsinchu 300, Taiwan
e-mail: cheinway@mail.nctu.edu.tw; cheinway@gmail.com

U. Hugentobler
Institut für Astronomische und Physikalische Geodäsie,
Technische Universität München, Arcisstr. 21,
80333 Munich, Germany

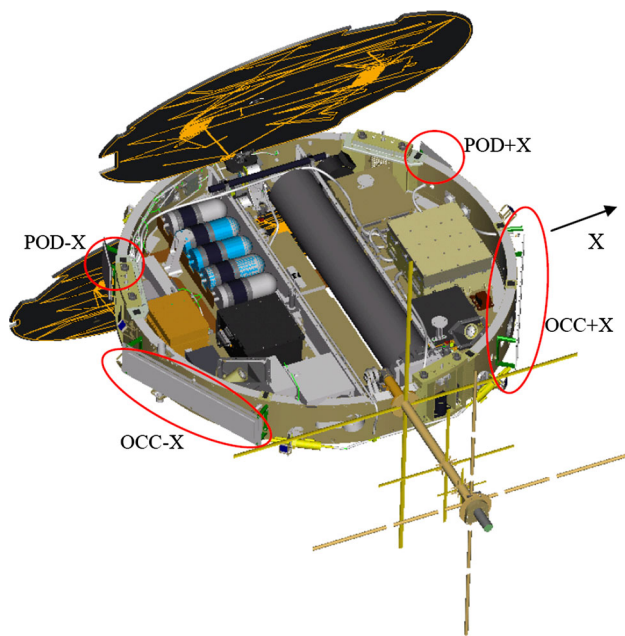


Fig. 1 COSMIC satellite configuration and GPS antennas for precise orbit determination (POD) and for occultation (OCC) (courtesy of NSPO)

(JPL). An earlier preflight test of the IGOR receivers was conducted by Montenbruck et al. (2006) using simulated GPS signals. In addition, the first-generation BlackJack GPS receiver with an ultra-stable quartz oscillator (USO) was installed on the GRACE satellite mission. The USO provides a frequency reference for both K-Band ranging (KBR) and GPS ranging measurements (Bettadpur 2012).

For a precise satellite orbit solution, the typical techniques are the reduced-dynamic orbit determination (DOD) and kinematic orbit determination (KOD) approaches. The Bernese 5.0 (Dach et al. 2007) GPS software offers the possibility to use these two approaches with GPS undifferenced observations. Sample studies using the DOD and KOD approaches with Bernese 5.0 for the CHAMP, GRACE, and COSMIC missions can be found in Švehla and Rothacher (2003), Jäggi et al. (2007), and Hwang et al. (2009). Typically, the receiver clock correction with respect to the GPS clock is estimated as part of the satellite orbit determination.

Compared to the POD antenna and GPS receiver of GRACE, there are a number of problems in POD using the data collected by the COSMIC antennas. We will analyze two of the problems: The antenna FOV and the clock stability of COSMIC. According to Hwang et al. (2010), the FOV of COSMIC POD antenna is about 120° , compared to 180° for GRACE. We will assess the FOV problem caused by the limited FOV of COSMIC in terms of post-fit phase residuals using a one-antenna orbit solution (one-AOS) and a two-antenna orbit solution (two-AOS). COSMIC's receiver clock stability has not been investigated in detail before,

and this problem will be studied here. In fact, the clock stability of GPS-equipped LEO will affect the accuracy of satellite orbit. First, a time–frequency spectral analysis will be carried out to detect clock anomalies and characterize the clock stability in different noise categories (Galleani 2008). Then, the modified Allan deviation (Allan 1987) will be used to determine the clock stability of COSMIC. From these two investigations for COSMIC, lessons for the GNSS payload of the COSMIC-2 satellite (Fong et al. 2011) will be highlighted. COSMIC-2 is a joint Taiwan–US mission for radio occultation (RO) applications and will consist of 13 satellites. The first six satellites will be deployed in 2016, followed by another seven satellites in 2018. Due to the large data volume of COSMIC observations, only GPS data on selected days will be used for our analyses.

Assessing FOV of COSMIC POD antenna

In this section, we assess the FOV of COSMIC POD antenna using the one-AOS and two-AOS in terms of the post-fit phase residuals. In the least-squares estimation of orbit and clock correction, the weighted quadratic form of phase residuals is a part of the target function that is minimized. Our assessment is summarized as follows:

(1) The orbit derived from the default antenna (POD-X in this case) orbit solution based on the reduced-dynamic approach was used to derive the GPS observation residuals of the non-default antenna (POD + X). The a priori orbit has to be precisely given by the default antenna orbit solution since less than 4 GPS satellites are tracked by the non-default antenna. This is the one-AOS from which we obtained the phase residuals of POD-X and POD + X antennas (Fig. 2a, b).

(2) The GPS observations from two POD antennas were used together to estimate the COSMIC orbit along with two receiver clocks in order to expand the total FOV. This is the two-AOS, which simultaneously produces the phase residuals of two antennas (Fig. 2c, d).

Figure 2a–d show the sky plots of phase residuals for FM4 from the one-AOS and two-AOS, and Fig. 2e and f the phase residuals for GRACE-A and B satellites, which have only one POD antenna. The 90° elevation corresponds to the normal of the POD antenna for both COSMIC and GRACE, which points to the $-Z$ direction of the spacecraft frame. The azimuth increases from 0° to 360° clockwise. The residuals from the azimuth of 330° to 30° in Fig. 2a are slightly degraded as compared to those in Fig. 2c. However, the residuals from the azimuth of 150° to 210° in Fig. 2d are slightly smaller than those in Fig. 2b. In this case, the standard deviations (STDs) of phase residuals for POD-X and POD + X antennas are 1.41 and 1.44 cm from the one-AOS, and 1.65 and 1.09 cm from the two-AOS. In

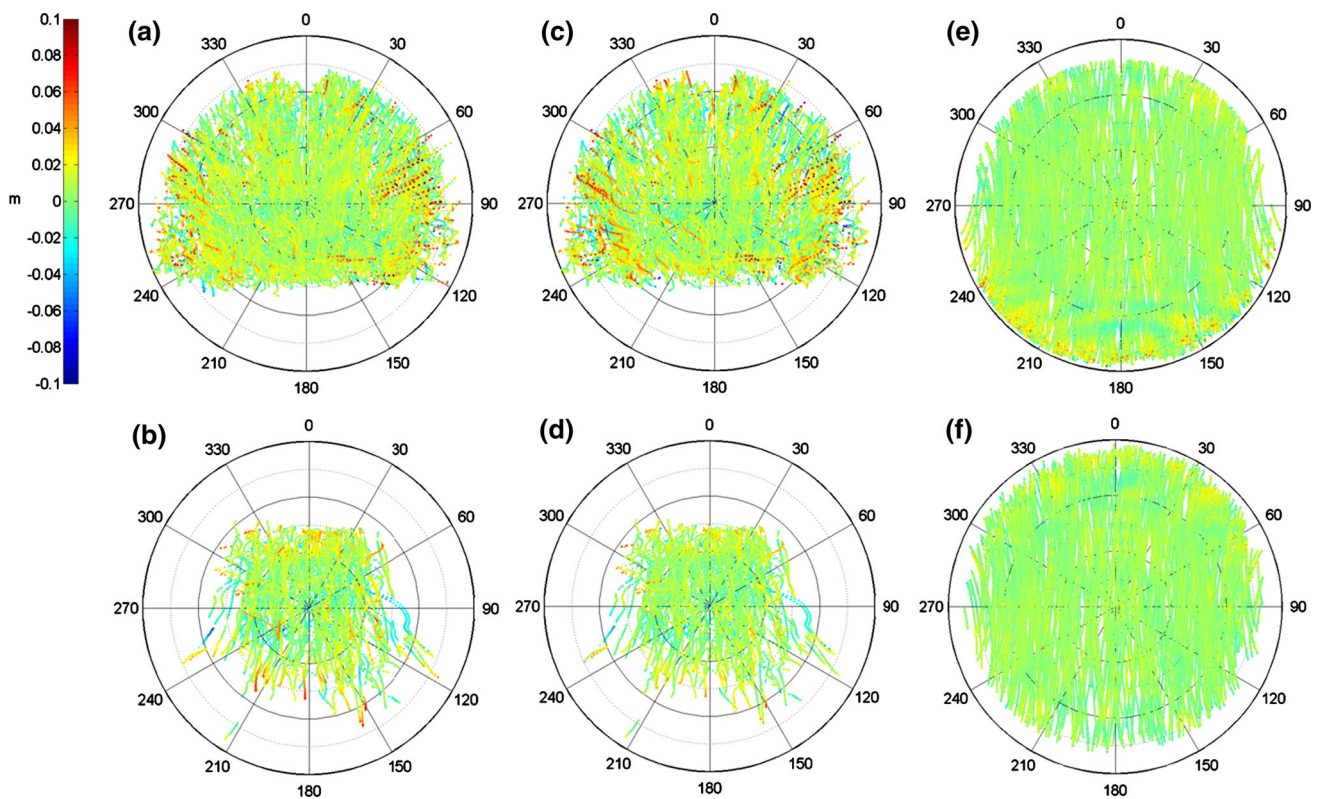


Fig. 2 Sky plots of phase residuals for FM4 on DOY 300, 2009 using **a** POD-X with one-AOS, **b** POD + X with one-AOS, **c** POD-X with two-AOS and **d** POD + X with two-AOS, and the sky plots for **e** GRACE-A (DOY 365, 2008) and **f** GRACE-B (DOY 365, 2008)

comparison with POD-X and POD + X of COSMIC, the antenna boresight of GRACE points to the zenith direction of the satellite body (Montenbruck et al. 2009). The zenith pointing of GRACE contributes partly to the smaller STDs of 0.70 and 0.57 cm for the A and B satellites. In conclusion, either the one-AOS or two-AOS of COSMIC yields STDs larger than the values from GRACE, and the use of GPS from two COSMIC POD antennas do not significantly reduce phase residuals.

Table 1 shows the daily mean numbers of GPS observations (MGO) and the daily STDs of phase residuals for POD-X and POD + X antennas of FM4 based on the one-AOS and two-AOS over DOY 300-307, 2009. The epoch (time) interval is 10 s, corresponding to a GPS sampling rate of 0.1 Hz. For comparison, the STDs of phase residuals of GRACE are at the millimeter level, based on 300 days of data (Hwang et al. 2010). For the POD-X antenna, the STDs from the two-AOS are about 3 mm larger than those from the one-AOS. However, for the POD + X antenna, the STDs from the two-AOS are 5 mm smaller than those from the one-AOS. In the one-AOS, the orbit derived from POD-X with about 6–7 observations per epoch is used to derive the residuals of POD + X, so the STDs of residuals associated with POD-X are smaller than those with POD + X. In comparison, about 8–9 observations from the two antennas are used to estimate the two-AOS orbit, which

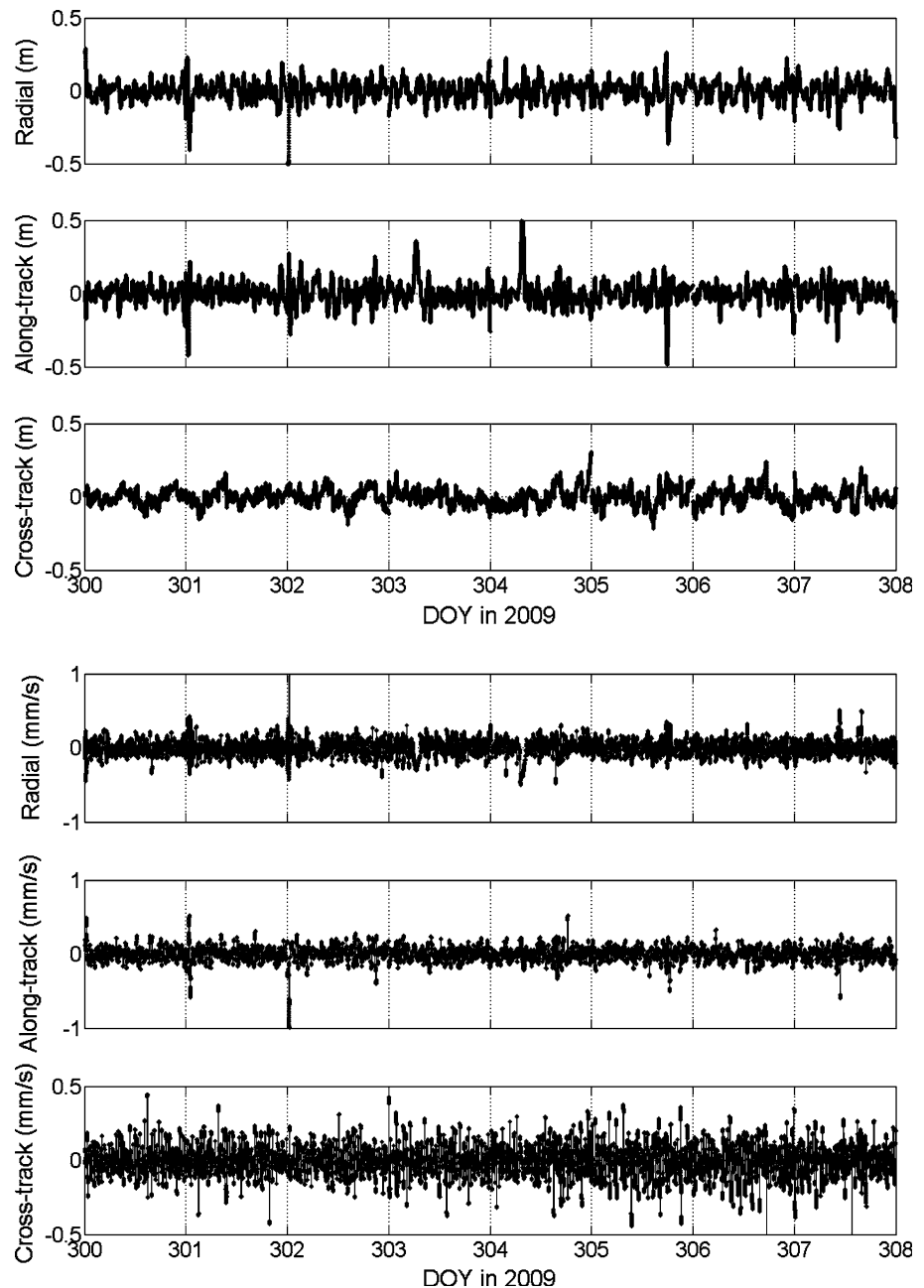
slightly changes the one-AOS orbit by adding the observations from POD + X. This is why we saw the few millimeter increase and decrease in POD-X and POD + X when the two-AOS is used.

Figure 3 shows the differences in position and velocity between the orbits of FM4 derived from the one-AOS and two-AOS. The mean value of the orbit differences was approximately zero from this experiment. Table 2 shows the daily STDs of differences in position and velocity for FM4 between the one-AOS and two-AOS. Overall, the orbit differences range from 5 to 9 cm, from 5 to 10 cm, and from

Table 1 Daily mean number of GPS observations (MGO) and STD values (in cm) of phase residuals for POD-X and POD + X antennas of FM4 based on the one-AOS and two-AOS

DOY 2009	One-AOS		Two-AOS		Two-AOS		MGO
	POD + X	MGO	POD-X	MGO	POD + X	POD-X	
300	1.44	2.57	1.41	6.69	1.09	1.65	9.26
301	1.78	2.53	1.67	4.98	1.33	1.95	7.51
302	1.93	2.43	1.80	5.27	1.33	2.14	7.70
303	1.89	2.57	1.72	6.15	1.39	2.04	8.72
304	1.80	2.55	1.75	6.28	1.31	2.09	8.83
305	1.85	2.59	1.53	5.93	1.32	1.89	8.52
306	1.89	2.56	1.45	5.49	1.43	1.81	8.05
307	1.73	2.58	1.49	5.66	1.29	1.79	8.24

Fig. 3 Differences between one-AOS and two-AOS in position (top) and velocity for FM4 (DOY 300–307, 2009)



4 to 7 cm in the radial, along-track and cross-track directions, respectively, and the velocity differences are consistent at the submillimeter level. The orbit differences in the along-track direction are relatively large as compared to the other two components. As expected in a typical reduced-dynamic solution, the differences in the cross-track direction are smaller than the others. Additionally, according to Kuang et al. (2008), GPS data from both POD antennas were used to estimate the COSMIC orbit along with a receiver clock. In that paper, the internal orbit accuracy showed a good agreement at the centimeter level with that given by Hwang et al. (2009). This means that no significant

difference between the COSMIC orbits derived from the one-AOS and two-AOS is found (Tables 1, 2). The result of this experiment shows the weakness of the COSMIC POD antennas in the GPS observation geometry and the need to place the COSMIC-2 antenna at the zenith direction.

Assessing the stabilities of COSMIC and GRACE receiver clocks

The COSMIC mission is mainly designed for the GPS-RO research, and thus, the atmospheric excess phase

Table 2 Daily STDs of differences in position and velocity for FM4 between the one-AOS and two-AOS

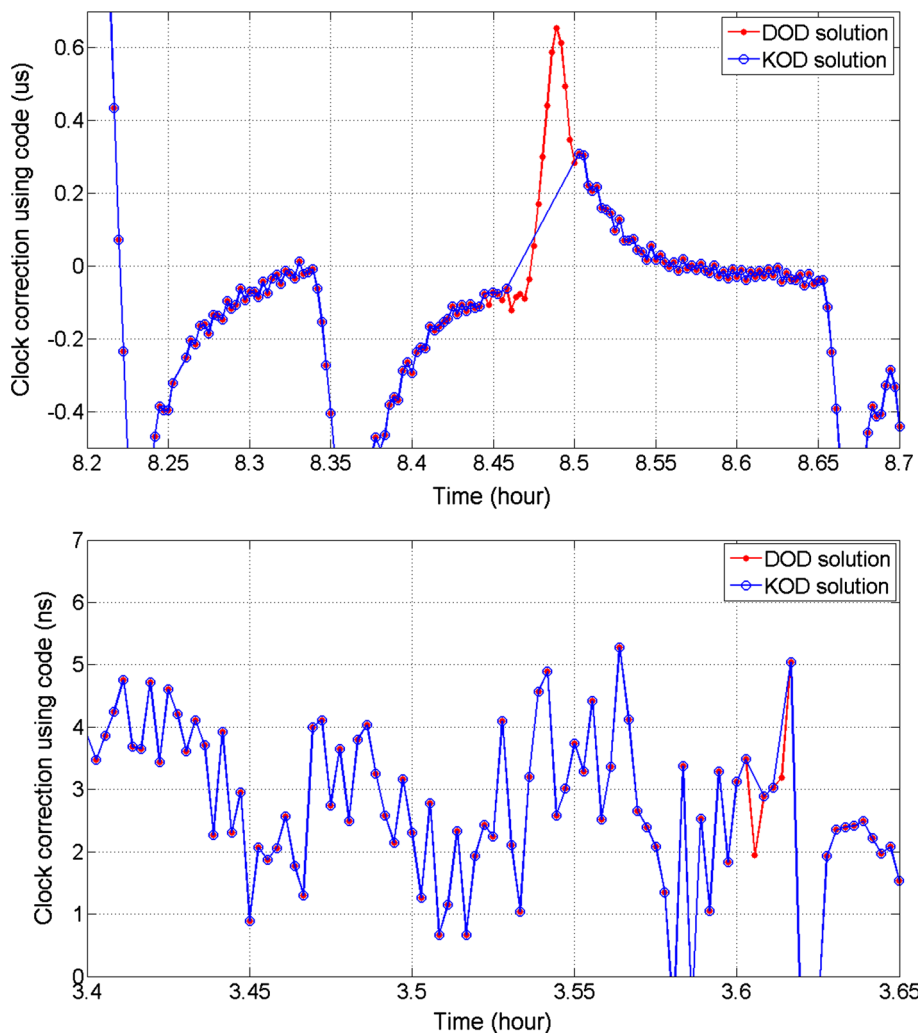
DOY 2009	Position (cm)			Velocity (mm/s)		
	Radial	Along-track	Cross-track	Radial	Along-track	Cross-track
300	5.92	5.91	4.31	0.09	0.09	0.10
301	7.76	7.83	4.78	0.10	0.10	0.10
302	9.23	8.75	5.93	0.14	0.13	0.09
303	6.65	8.73	4.55	0.11	0.09	0.11
304	6.52	10.65	7.48	0.12	0.10	0.11
305	7.79	8.37	6.29	0.08	0.10	0.12
306	6.60	6.69	6.65	0.08	0.08	0.12
307	7.43	7.52	5.52	0.09	0.09	0.11

derived from the POD result is crucial for the retrieval of atmospheric profile. The quality of excess phase is mainly associated with the quality of receiver clock. Here, we will show a comparison in clock between the IGOR-clock-derived and USO-clock-derived orbit solutions.

Receiver clock estimation using code and phase observations

In addition to the limited FOV, the degraded COSMIC orbit accuracy can also be caused by degraded GPS data of COSMIC, which is in turn related to the stability of the

Fig. 4 Receiver clock corrections using code observations for FM1 (microsecond level) (DOY 125, 2008;top) and GRACE-A (nanosecond level) (DOY 174, 2007) based on both DOD and KOD



receiver clock. Sample studies of the relation between receiver clock quality and GPS positioning accuracy are given in Yeh et al. (2009, 2012). Figure 4 shows the estimated receiver clock correction using code observations from FM1 and GRACE-A using the reduced-dynamic and kinematic methods (DOD and KOD). The difference in the clock patterns between FM1 and GRACE-A is caused by the change of GPS geometry from one epoch to another. While the FM1 clock corrections change rapidly, those of GRACE-A are quite smooth. There is a sharp difference in the magnitude of clock correction: The clock correction of FM1 is at the microsecond level, compared to the nanosecond level of GRACE. The need of requiring more than four tracked GPS satellites in the KOD solution often leads to gaps in clock estimation. For example, at around 8.5 h in Fig. 4 (top) and 3.6 h in Fig. 4 (bottom), insufficient numbers of tracked GPS satellites in the KOD solution (blue line) result in singularities in the normal equations. In contrast, such singularities did not occur in the DOD

solution (red line) because the DOD approach removes the deficiency in the GPS geometry using force modeling and orbit integration.

We also used phase observations to estimate clock corrections. Figure 5 shows the phase-derived clock corrections for FM6 and GRACE-A based on the DOD and KOD approaches. The magnitude of the phase-derived clock correction for COSMIC is similar to the code-derived result given in Fig. 4 since the both are at a level of microsecond. Again, the difference in the clocks between the DOD and KOD solutions is caused by the two different orbit determination procedures. In Fig. 5, we clearly see discontinuities of few nanoseconds near the integer days in the estimated clock of GRACE-A. This is because two consecutive orbit arcs are jointed at 0 h UTC. The discontinuities of the COSMIC clocks are overwhelmed by the large noises in the phase observations. Several methods can be used to reduce the discontinuity at the arc boundary, for example, ambiguity stacking and clock handover (Dach et al. 2006), and ambiguity estimation using

Fig. 5 Phase-derived clock corrections of FM6 (DOY 256–258, 2010; top) and **b** GRACE-A (DOY 329–331, 2008) based on DOD (red) and KOD (blue) orbit solutions

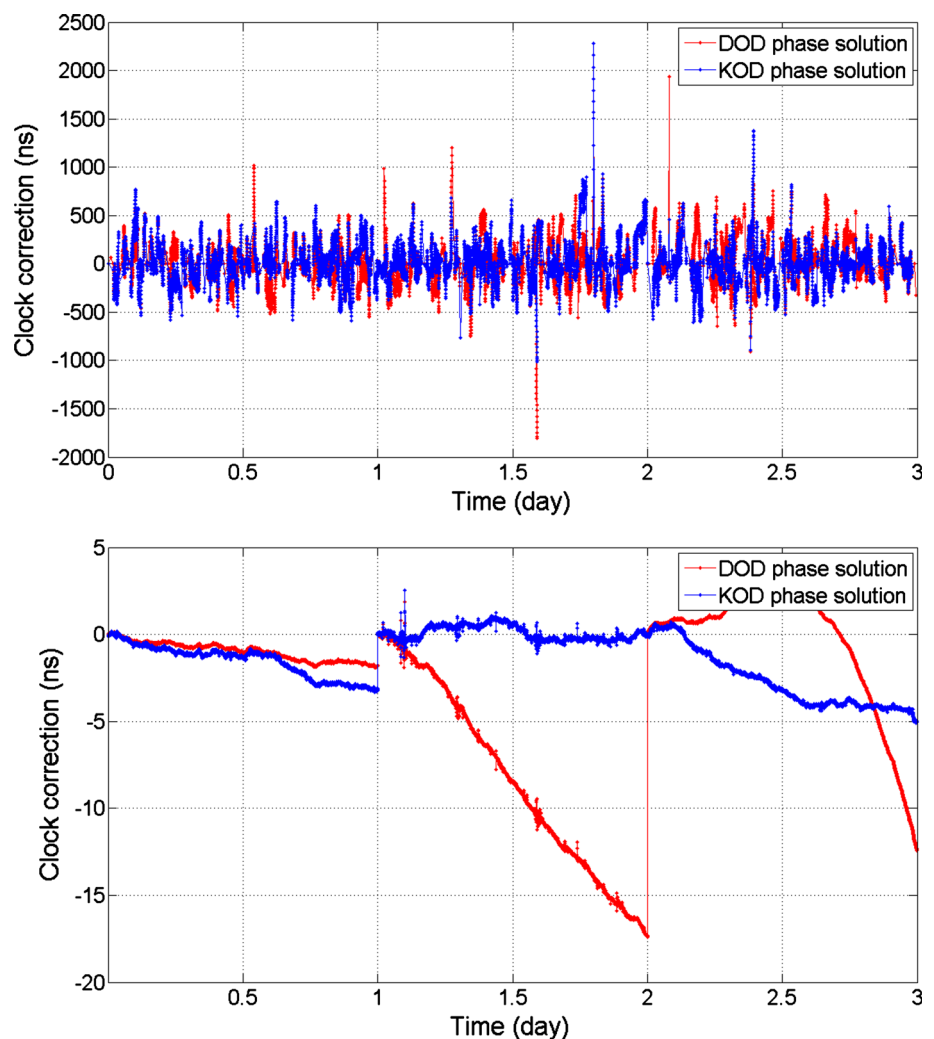


Table 3 Average TDOP (in ns) from DOD and KOD solutions using 10-day COSMIC and GRACE-A GPS data

	FM1	FM2	FM3	FM4	FM5	FM6	GRACE-A
DOD	0.055	0.041	0.050	0.031	0.055	0.026	0.014
KOD	0.066	0.078	0.067	0.062	0.087	0.075	0.024

undifferenced phases (Delporte et al. 2008). Because our focus is on the clock behavior of the daily solutions, methods to reduce the discontinuity in clock are not pursued here.

Figure 5 shows the magnitude of clock correction of FM6 is about few hundreds of nanoseconds and is much larger than that of GRACE-A. The magnitude for the FM6 clock correction is similar to the result given by Montenbruck et al. (2006; Table 3). The effects due to phase multipath (Hofmann-Wellenhof et al. 2001, p. 92), phase wind-up (Tseng et al. 2012) and ionospheric delay (Hwang et al. 2010), and large time dilution of precision (TDOP) amount to only few nanoseconds at most. Because the magnitudes of the COSMIC clock corrections are at the one hundred nanosecond level, these four effects are minor.

Because a detailed analysis of COSMIC TDOP has not been given before; here, we show the phase-derived TDOP values from variance–covariance matrices from orbital solutions. Table 3 shows the averaged TDOP from the DOD and KOD solutions for satellites FM1-FM6 and GRACE-A over 10 days. Note that, different 10-day periods are used in Table 3: DOY 330-339, 2008 for FM1; DOY 330-339, 2008 for FM2; DOY 110-119, 2008 for FM3; DOY 110-119, 2008 for FM4; DOY 210-219, 2008 for FM5; DOY 210-219, 2008 for FM6; DOY 170-179, 2007 for GRACE-A. From the DOD solution, FM6 has a smaller TDOP compared to the other COSMIC satellites. However, the TDOP of 0.026 ns for FM6 is still larger than the value of 0.014 ns for GRACE-A. This suggests that the GPS geometry strength of COSMIC is weaker than that of GRACE. Again, due to the need of at least four tracked GPS satellites, the TDOP values from KOD are larger than those from DOD. The limited FOV of COSMIC worsens the KOD-derived TDOP by reducing the number of tracked GPS satellites. In conclusion, the GPS clock stability and data quality of COMIC should be greatly improved to achieve the performance of GRACE. In order to avoid large uncertainties and gaps in clock estimation, we will use the clock corrections estimated from DOD using phase observations in the analysis of clock stability given below.

Time–frequency spectrum of clock and clock stability

A time–frequency spectrum shows the variations of signal components varying with time. Figure 6 shows the time–frequency spectra of the phase-derived clock corrections

for FM6 and GRACE-A (Sect. 3.1), based on the formulae given in Galleani (2008). In general, the spectrum of COSMIC at a given epoch decreases with frequency (top panel), and COSMIC’s overall spectra are much larger than the spectra of GRACE-A (bottom panel). The likely causes of the large spectra of COSMIC clocks are the instability of receiver clock (see below), TDOP, phase multipath, phase wind-up, and high-order ionospheric terms. The spectra of COSMIC at the frequencies of 0–0.005 Hz contain significant powers, which appear to be proportional to the inverses of frequency and squared frequencies, and are likely to fall into the categories of flicker and random walk noises (Riley 2003). However, the 1-day record length in Fig. 6 is too short to separate the flicker and random walk components, and a detailed modeling of the noise characteristics is needed before reaching a conclusion. In comparison, the powers at the frequencies of 0–0.005 H in the GRACE-A spectrum are relatively low. We believe that the GRACE low clock noise is attributed to its high-quality USO-based clock.

The time–frequency spectrum in Fig. 6 (top) points out the high-noise problem of the COSMIC clock. To quantify this problem, we computed the clock stability using the modified Allan deviation, $\sigma_y(\tau)$, as (Allan 1987)

$$\sigma_y(\tau) = \left\{ \frac{1}{2\tau^2 n^2 (N - 3n + 1)} \sum_{j=1}^{N-3n+1} \left(\sum_{i=j}^{n+j-1} ((\Delta\delta_{i+2n} - \Delta\delta_{i+n}) - (\Delta\delta_{i+n} - \Delta\delta_i)) \right)^2 \right\}^{1/2} \tag{1}$$

where $\Delta\delta_i$ denotes the phase-derived clock correction with i being the index of epoch, N is the number of $\Delta\delta_i$, $\tau = n\tau_0$ is the averaging time window with τ_0 being the interval between two consecutive $\Delta\delta_i$, and n is a number to determine the length of τ . Fig. 7 shows the clock stabilities of FM6 and GRACE-A for the 1-day phase-derived clock from DOD, with n ranging from 10 to 10^4 . According to (1), the clock stability is mainly governed by the values of the pairs $(\Delta\delta_{i+2n} - \Delta\delta_{i+n})$ and $(\Delta\delta_{i+n} - \Delta\delta_i)$, which are related to the stability in estimating the receiver clock correction (Fig. 5). The clock stabilities for FM6 range from 10^{-9} to 10^{-11} for $\tau = 10$ to 10^4 s, compared to 10^{-12} – 10^{-14} for GRACE-A. For $\tau = 10$ s, such clock stabilities correspond to decimeter and submillimeter errors in GPS ranging measurements for COSMIC and GRACE, respectively. Note that, the stability of GRACE clock in Fig. 7 agrees well with the result stated in Bettadpur (2012; p. 14). The decimeter-level error in GPS ranging measurements of COSMIC caused by the receiver clock instability belong to systematic errors, which are absorbed by parameters such as the six Kepler elements and pseudo-

Fig. 6 Time-frequency spectra of phase-derived clock corrections for FM6 (DOY 256, 2010; top) and GRACE-A (DOY 329, 2008)

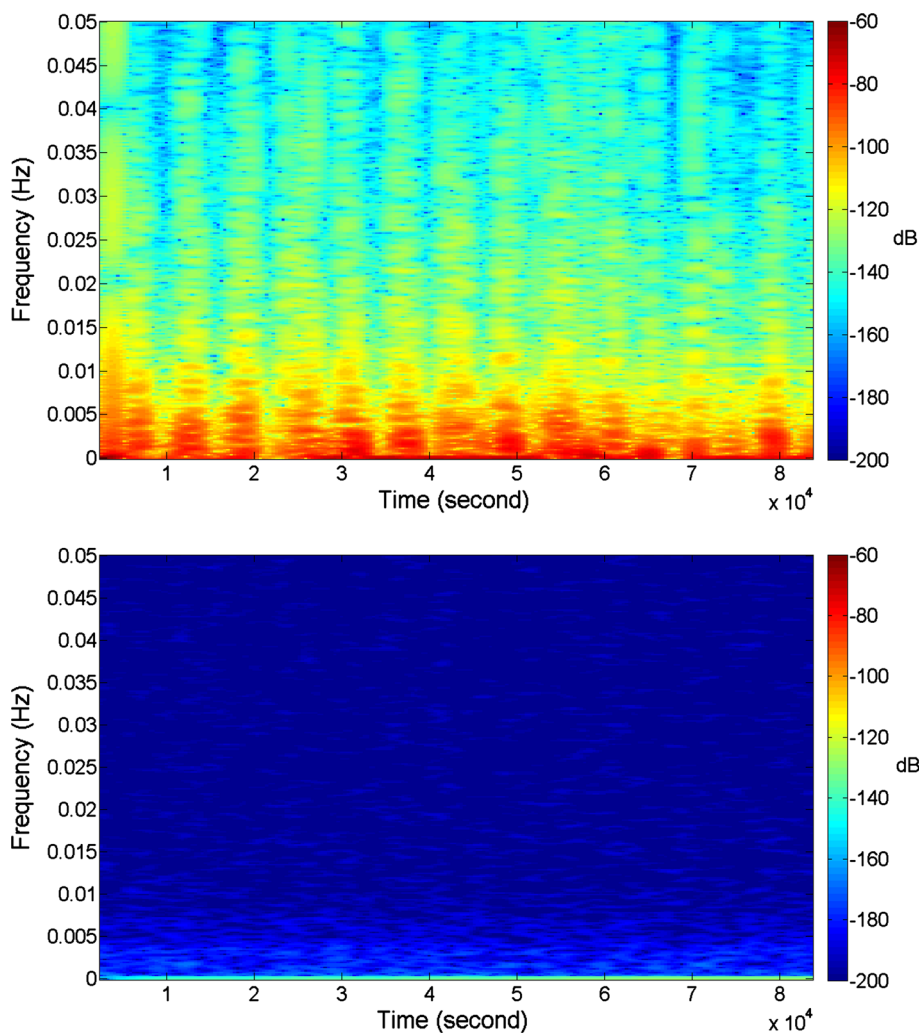
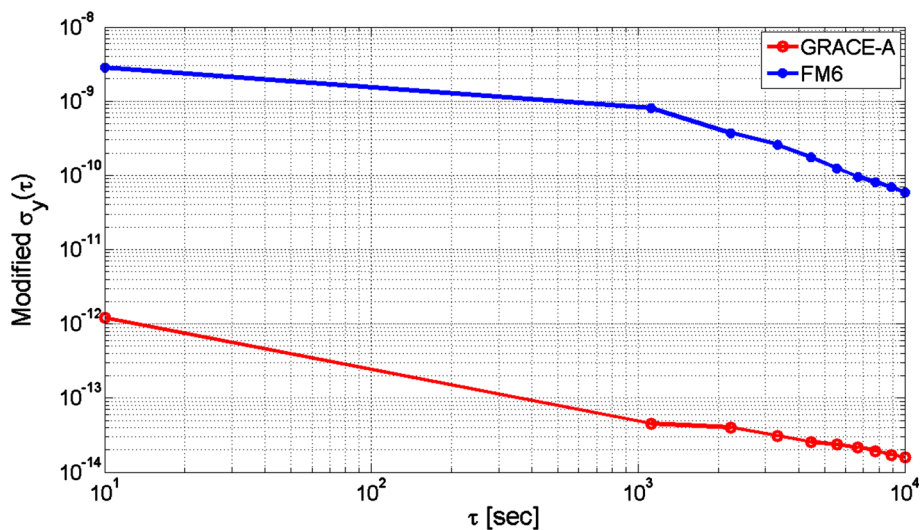


Fig. 7 Clock stabilities of FM6 (DOY 256, 2010) and GRACE-A (DOY 329, 2008) computed from the phase-derived clock corrections



stochastic pulses in orbit determinations. As a result, the phase residuals of COSMIC are at the centimeter level (Table 1).

As a final remark, we discuss the effect of clock stability on deriving atmospheric excess phase from occulted GPS signals. In the GPS-RO literature, both single-differenced

Table 4 Recommended improvement of scientific payloads for COSMIC-2 over COSMIC

Item	COSMIC	COSMIC-2
<i>Positioning requirement</i>		
FOV	120°	180°
Antenna orientation	Titled 15° from the zenith	Exact zenith
SLR retro-reflector	No	Yes
<i>Att. control requirement</i>		
Attitude sensors	Earth sensor, Sun sensor, and magnetometer	Gyro and star tracker
Roll, pitch, yaw	2°, 1°, 2° (1-sigma)	1°, 1°, 1° (3-sigma)
<i>Receiver requirement</i>		
Receiver	IGOR	TriG
Navigation satellite	GPS	GNSS
CPU	1	2 (1 for POD; 1 for RO)

phases and undifferenced phases have been used to derive excess phases. Sample studies in the two cases are given by Schreiner et al. (2010) and Beyerle et al. (2005), respectively. In theory, the use of single-differenced phases can remove the errors in the receiver clock, which need to be modeled when using undifferenced phases. However, Beyerle et al. (2005) show that the refractivity obtained from the GRACE excess phase based on undifferenced phases contains less biases than that based on single-differenced phases. Beyerle et al. (2005) attribute the result with undifferenced phases to the high-quality, USO-controlled GRACE clock. In fact, single-differenced phases introduce extra noise to excess phase when differencing phases from the LEO to the occulting GPS satellite and the referencing GPS satellite. With a GRACE-grade clock in future COSMIC-2 GNSS receivers, it is possible to determine excess phase with undifferenced phases to reduce biases in atmospheric parameters.

Lessons for COSMIC-2

The result from the analyses of the COSMIC FOV and clock stability will provide a key reference for the approved COSMIC-2 mission. In Table 4, we recommend selected improvements of COSMIC-2 in orbit and clock solution based on the results of this research and Tseng et al. (2012). A detailed description for Table 4 is as follows:

1. For satellite orbit determination, the orientation of the POD antenna should be pointed in the zenith direction. The FOV of COSMIC-2 should be increased to near 180° in order to yield a better GNSS visibility geometry and signal quality, and to mitigate the higher-order ionospheric effect on the orbit determination. Based on the results of Jäggi et al. (2009), Montenbruck et al. (2009) and Bock et al. (2011), phase center variation (PCV) maps from onboard GNSS observations of

- COSMIC and COSMIC-2 should be used for POD, instead of the preflight calibrated one. In addition, a satellite laser ranging (SLR) retro-reflector can be mounted on COSMIC-2, and the SLR measurements can be used to validate the GPS-based orbits. The root-mean-square (RMS) differences between the SLR measurements and orbits can be an indicator of orbit accuracy. A further application of SLR measurements of the COSMIC-2 satellite constellation is to estimate the geocenter motion to improve the ITRF realization.
2. For attitude control, more accurate attitude sensors, such as gyro and star tracker sensors, should be used in COSMIC-2 satellites instead of the earth sensor, the Sun sensor, and the magnetometer. The requirement of attitude measurement for COSMIC-2 should be 1° for roll, pitch, and yaw (3-sigma). In comparison, the current accuracies (1-sigma) of COSMIC attitude measurement are 2°, 1°, and 2° in roll, pitch, and yaw, respectively. The poor attitude control is a factor that degrades the COSMIC POD (Tseng et al. 2012).
 3. For receiver performance, the latest BlackJack receiver TriG (Esterhuizen et al. 2009) should be used on COSMIC-2. A TriG receiver is a GNSS receiver capable of receiving GPS, GLONASS, and GALILEO signals. Two CPUs in the TriG receiver will be used to separately deal with the large volume of POD and GPS-RO data. The clock of a TriG receiver will be expected to reduce the noise in raw GPS observation, as compared to the clock on COSMIC. Observations from a multi-GNSS should be used to improve the COSMIC-2 orbit and clock solution.

Conclusions

We provide suggestions for the approved COSMIC-2 satellite mission in FOV and clock stability of its GNSS

receiver. The narrow FOV of COSMIC affects the length of tracked GPS arcs and in turn degrades its orbit accuracy. This narrow FOV results in GPS observations at low-elevation angles at the COSMIC POD antennas. Such low-elevation signals might be affected by the higher-order ionospheric terms, which are on the order of submillimeter to centimeter (Kedar et al. 2003). Since low-elevation GPS observations are also complicated by factors such as large ionospheric delay and severe multipath effect. They will not effectively enhance the orbit solution, even if a smaller weight is assigned to them. As such, we use a uniform weight for all COSMIC GPS observations. Furthermore, the instability of COSMIC receiver clock results in decimeter-level errors in GPS ranging measurements, which reduces the quality of atmospheric excess phase and in turn the quality of atmospheric parameters retrieved from occulting profiles between COSMIC and GPS. With an improved GNSS payload performance as suggested in Table 4 and a larger number of satellites in the COSMIC-2 constellation of up to 13, we expect that COSMIC-2 will deliver improved satellite orbits and improved atmospheric parameters over COSMIC.

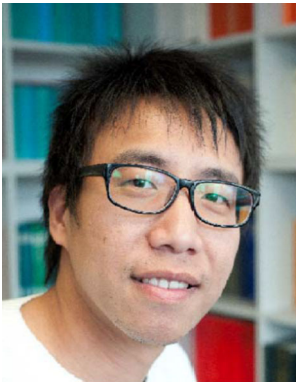
Acknowledgments This research is supported by National Space Organization, Taiwan (contract no. NSPO-S-100011), Australia Space Research Program (ASRP) (Grant No. ASRP2, RMIT), and National Science Council (contract no. 100-2221-E-009-132-MY3). We thank CODE for providing the precise GPS orbit, clock, and earth rotation parameters and are grateful to the comments of reviewers to enhance the quality of the paper.

References

- Allan DW (1987) Time and frequency (time-domain) characterization, estimation, and prediction of precision clock and oscillators. *IEEE Trans Ultrason Ferroelect Freq Contr*, vol.uffc-34(6)
- Bettadpur S (2012) GRACE Product Specification Document, Rev. 4.6. Technical Report GRACE 327-720 (CSR-GR-03-02), Center for Space Research, The University of Texas at Austin
- Beyerle G, Schmidt T, Michalak G, Heise S, Wickert J, Reigber C (2005) GPS radio occultation with GRACE: Atmospheric profiling utilizing the zero difference technique. *Geophys Res Lett* 32:L13806. doi:10.1029/2005GL023109
- Bock H, Jäggi A, Meyer U, Dach R, Beutler G (2011) Impact of GPS antenna phase center variations on precise orbits of the GOCE satellite. *Adv Space Res* 47(11):1885–1893. doi:10.1016/j.asr.2011.01.017
- Dach R, Schildknecht T, Hugentobler U, Bernier L-G, Dudle G (2006) Continuous geodetic time transfer analysis methods. *IEEE Trans Ultrason Ferroelect Freq Contr* 53:1250–1259
- Dach R, Hugentobler U, Fridez P, Meindl M (2007) Bernese GPS Software—Version 5.0, Astronomical Institute, University of Bern, Switzerland
- Delporte J, Mercier F, Laurichesse D, Galy O (2008) GPS carrier-phase time transfer using single-difference integer ambiguity resolution. *Int J Navig Obs*. doi:10.1155/2008/273785
- Esterhuizen S, Franklin G, Hurst K, Mannucci A, Meehan T, Webb F, Young L (2009) TriG—A GNSS precise orbit and radio occultation space receiver. 22nd International meeting of the satellite division of the institute of navigation, Savannah, GA, September 22–25, page(s):1442–1446
- Fong CJ, Yang SK, Chu CH, Huang CY, Yeh JJ, Lin CT, Kuo TC, Liu TY, Yen NL, Chen SS, Kuo YH, Liou YA, Chi S (2008) FORMOSAT-3/COSMIC constellation spacecraft system performance: after 1 year in orbit. *IEEE Trans Geosci Remote Sens* 46:3380–3394
- Fong CJ, Whiteley D, Yang E, Cook K, Chu V, Schreiner B, Ector D, Wilczynski P, Liu TY, Yen N (2011) Space and ground segment performance and lessons learned of the FORMOSAT-3/COSMIC mission: 4 years in orbit. *Atmos Meas Tech* 4:1115–1132. doi:10.5194/amt-4-1115-2011
- Galleani L (2008) Detection of changes in clock noise using the time-frequency spectrum. *Metrologia* 45:S143–S153. doi:10.1088/0026-1394/45/6/S20
- Hofmann-Wellenhof B, Lichtenegger H, Collins J (2001) Global positioning system: theory and practice. Springer Wien New York, ISBN 3-211-83472-9
- Hwang C, Tseng TP, Lin T, Švehla D, Schreiner B (2009) Precise orbit determination for the FORMOSAT-3/COSMIC satellite mission GPS. *J Geod* 83:477–489. doi:10.1007/s00190-008-0256-3
- Hwang C, Tseng TP, Lin T, Švehla D, Hugentobler U, Chao BF (2010) Quality assessment of FORMOSAT-3/COSMIC and GRACE GPS observables: analysis of multipath, ionospheric delay and phase residual in orbit determination. *GPS Solut* 14(1):121–131. doi:10.1007/s10291-009-0145-0
- Jäggi A, Hugentobler U, Bock H, Beutler G (2007) Precise orbit determination for GRACE using undifferenced or doubly differenced GPS data. *Adv Space Res* 39(10):1612–1619. doi:10.1016/j.asr.2007.03.012
- Jäggi A, Dach R, Montenbruck O, Hugentobler U, Bock H, Beutler G (2009) Phase center modeling for LEO GPS receiver antenna and its impact on precise orbit determination. *J Geod* 83:1145–1162. doi:10.1007/s00190-009-0333-2
- Kedar S, Hajj GA, Wilson BD, Heflin MB (2003) The effect of the second order GPS ionospheric correction on receiver positions. *Geophys Res Lett* 30(16):1829. doi:10.1029/2003GL017639
- Kuang D, Bertiger W, Desai S, Haines B, Iijima B, Meehan T (2008) Precise orbit determination for COSMIC Satellites using GPS data from two on-board Antennas. Proceedings of the IEEE/ION PLANS, pp 720–730, May 6–8, Monterey, California
- Montenbruck O, Garcia-Fernandez M, Williams J (2006) Performance comparison of semicodeless GPS receivers for LEO satellites. *GPS Solut* 10:249–261. doi:10.1007/s10291-006-0025-9
- Montenbruck O, Garcia-Fernandez M, Yoon Y, Schön S, Jäggi A (2009) Antenna phase center calibration for precise positioning of LEO satellites. *GPS Solut* 13:23–34. doi:10.1007/s10291-008-0094-z
- Riley WJ (2003) Techniques for frequency stability analysis. *IEEE International Frequency Control Symposium*, Tampa, FL, May 4
- Schreiner W, Rocken C, Sokolovskiy S, Hunt D (2010) Quality assessment of COSMIC/FORMOSAT-3 GPS radio occultation data derived from single- and double-difference atmospheric excess phase processing. *GPS Solut* 14:13–22. doi:10.1007/s10291-009-0132-5
- Švehla D, Rothacher M (2003) Kinematic and reduced-dynamic precise orbit determination of low earth orbiters. *Adv Geosci* 1:47–56

- Tseng TP, Hwang C, Yang SK (2012) Assessing attitude error of FORMOSAT-3/COSMIC satellites and its impact on orbit determination. *Adv Space Res* 49(9):1301–1312. doi:10.1016/j.asr.2012.02.007
- Yeh TK, Hwang C, Xu G, Wang CS, Lee CC (2009) Determination of global positioning system (GPS) receiver clock errors: impact on positioning accuracy. *Meas Sci Technol* 20(7):1–7. doi:10.1088/0957-0233/20/7/075105
- Yeh TK, Chen CH, Xu G, Wang SC, Chen KH (2012) The impact on the positioning accuracy of the frequency reference of a GPS receiver. *Surv Geophys*. doi:10.1007/s10712-012-9202-2

Author Biographies



Dr. Tzu-Pang Tseng is an assistant research fellow in GPS Science and Application Research Center (GPSARC) of National Central University of Taiwan. His expertise focuses on precise orbit determination of low earth orbiters, such as FORMOSAT-3/COSMIC and GRACE satellites. Currently, his research activity focuses on the POD-related calibration of the upcoming FORMOSAT-7/COSMIC-2 satellite using GNSS data.



Dr. Kefei Zhang is professor and director of the Satellite Positioning for Atmosphere, Climate and Environment (SPACE) Research Centre (<http://www.rmit.edu.au/SPACE>) and the Satellite Positioning and Navigation (SPAN) Laboratory at RMIT University. He has over 20 years of research experience in satellite positioning, geodesy and surveying. His primary research interest is development and application of GNSS/GPS technologies for high-accuracy position-

ing, atmospheric studies (e.g. for space weather, extreme weather events, space debris surveillance and collision warning, climate change, weather and environment), and people mobility and object tracking. He led an international research consortium and won a prestigious, multi-million-dollar Australia Space Research Program project in satellite positioning, space tracking and atmospheric studies for climate and space weather.



Dr. Cheinway Hwang received BS degree in surveying engineering from National Cheng Kung University in 1984, MS and PhD degrees in geodetic science in 1989 and 1991 from the Ohio State University. He was a postdoctoral research associate in the Department of Earth Sciences, Oxford University, 1991–1993. He is now chair professor, Department of Civil Engineering, National Chiao Tung University, Taiwan. He received Distinguished

Research Awards of National Science Council of Taiwan in 1998, 2000 and 2002. He is a fellow of International Association of Geodesy. His major research areas are satellite geodesy and gravimetry.



Dr. Urs Hugentobler is a professor at the Institute for Astronomical and Physical Geodesy of Technische Universität München, Germany, and head of the Research Facility Satellite Geodesy. His research activities include precise positioning using GNSS, precise orbit determination and modelling, reference frame realization, and time transfer. He is the current Chair of the International GNSS Service Governing Board.



Dr. Chuan-Sheng Wang received his BSc and MSc degrees from the Department of Civil Engineering, National Chiao Tung University, Taiwan in 1998 and 2000, respectively, and PhD in space sciences from National Central University, Taiwan in 2009. Upon completing his PhD, he was employed at RMIT University, Australia, as a research fellow. He is currently a postdoctoral research fellow in the Department of Real Estate and Built Environment, National Taipei University. His research interests include precise GNSS positioning, GNSS meteorology and GNSS Reflectometry.



Dr. Suelynn Choy completed her PhD in 2009 in the area of GPS Precise Point Positioning (PPP) at RMIT University, Australia. Since then, she works as a full-time academic staff at the School of Mathematical and Geospatial Sciences in RMIT University. She teaches land surveying, geodesy, and GNSS navigation to undergraduate and graduate students. Her current research interests are in the areas of multi-GNSS PPP and using GNSS for atmospheric

and ground remote sensing. Suelynn is the co-chair of the IAG (International Association of Geodesy) Working Group 4.5.2: PPP and Network RTK under Sub-Commission 4.5: High Precision GNSS Algorithms and Applications.



Yi-Shan Li received the BS degree in the Chung Cheng Institute of Technology from National Defense University and the MS degree in National Chiao-Tung University, in 2000 and 2004, respectively. She is working toward her PhD degree. Her research focuses on precise orbit determination (POD) of LEO satellites and GPS data processing. Currently, she is developing a real-time automatic POD system for FORMOSAT-3/COSMIC and FORMOSAT-7/

COSMIC-2 satellite missions.